HHS Public Access

Author manuscript

J Mater Chem B Mater Biol Med. Author manuscript; available in PMC 2017 September 22.

Published in final edited form as:

J Mater Chem B Mater Biol Med. 2016 ; 4(33): 5560–5566. doi:10.1039/C6TB01234E.

Bright and Stable Near-Infrared Pluronic-Silica Nanoparticles as a Contrast Agent for *in vivo* Optical Imaging

Lesan Yan[a], **Huiquan Wang**[b], **Anqi Zhang**[a], **Calvin Zhao**[a], **Yongping Chen**[a], and **Xingde Li**[*,a]

[a]Department of Biomedical Engineering, Johns Hopkins University, Baltimore, MD 21205

[b]School of Electronics and Information Engineering, Tianjin Polytechnic University, Tianjin, 3000387, China

Abstract

Near-infrared (NIR) fluorescent nanostructured materials have emerged as novel contrast agents for non-invasive bioimaging. Here we report a class of polymer-silica nanoparticles doped with a NIR fluorescent dye prepared through a facile one-pot strategy. Hydrophobic NIR fluorescent dyes such as IR 780 iodide could be easily encapsulated into the micellar core by self-assembly of amphiphilic triblock copolymer Pluronic F127. When subsequently adding silane in aqueous solution, nanoparticles with a cross-linked core and a hydrophilic PEG shell were formed. The structure of the as-obtained nanoparticles was confirmed by transmission electron microscopy (TEM) and dynamic light scattering (DLS). The nanoparticles exhibited a well-defined spherical structure with a mean diameter of approximately 30 nm, and excellent monodispersity and stability in aqueous solution. In addition, the photo-stability of IR 780 was significantly improved by encapsulation into the nanoparticles. *In vitro* MTT assay with cell lines HEK293 and A431 demonstrated that the IR 780 loaded nanoparticles (termed as IR780@NPs) were biocompatible. *In vivo* sentinel lymph node imaging revealed that the fluorescent intensity and retention time of the IR780@NPs were clearly superior to its constituent free dye, making it amenable to *in vivo* bioimaging. Further *in vivo* tumor imaging indicated that IR780@NPs have a longer retention time and much higher accumulation on the tumor site compared to free dye after intravenous administration. Overall this hydrophilic NIR fluorescent contrast agent exhibits excellent photophysical characteristics and low cytotoxicity, and holds a strong promise for a variety of applications including bioimaging and therapy.

1. Introduction

Optical imaging as a promising molecular imaging approach is being widely explored in the biomedical field, particularly in cellular and molecular biological imaging [1, 2], drug delivery [3, 4], image-guided surgery [5, 6] and lymph node mapping [7–9]. As one of the most important and powerful tools among conventional imaging techniques, fluorescence imaging offers significant advantages, including high resolution, high sensitivity and contrast, potential molecular specificity, noninvasiveness and *in vivo* real-time imaging capability [10, 11]. However, most of the current existing fluorescent imaging probes are in

* xingde@jhu.edu (Prof. Xingde Li).

the visible wavelength region with limited penetration depth and strong background autofluorescence in biological tissues [12]. As a result, development of NIR fluorescent probes has attracted significant interest due to reduced optical scattering and absorption and low tissue autofluorescence for light in the 700—1000 nm NIR region, making it possible to perform deep tissue imaging with a high signal-to-background ratio [13].

To develop an ideal NIR fluorescent probe for biomedical applications, several general criteria have to be met, such as photochemical stability, biocompatibility and *in vivo* half-life time. Free dyes, most known as small organic molecules, usually can be easily degraded in aqueous media and quickly cleared from the body [14], limiting the scope of their biomedical applications. As a consequence, development of novel NIR contrast agents with highly enhanced performance over free dyes has become a critical step to maximize the potential of *in vivo* fluorescent imaging. For the past decade, numerous efforts have been devoted to the synthesis of NIR fluorescent nanoparticles as contrast agents, such as quantum dots (QDs) and NIR fluorophore-doped polymeric nanoparticles [15–18]. To date, these kinds of NIR fluorescent nanoparticles have emerged as promising fluorescent probes alternatives to free dyes for *in vivo* applications, as they exhibit improved resolution and sensitivity, prolonged blood circulation time and potentially passive targeting effect in tumor tissue [19]. However, most QDs particularly the NIR QDs have potentially toxic elements in their cores, making biosafety a serious concern [20]. Polymeric nanoparticles are one of the most promising types employed for a wide range of *in vivo* applications [21] due to their high biocompatibility. However, these efforts fall short till now in improving the optical performance for deep-tissue imaging applications [22]. More recently, silica nanoparticles have emerged as an attractive platform for synthesizing NIR fluorescent probes because of its optical transparency in the NIR region, simple and affordable synthesis procedure as well as high stability and biocompatibility [23–29]. For example, Shi and coworkers produced efficient fluorescent probes for real time living cell imaging and endocytosis tracking using hydrophobic [27] and pH-responsive dyes [28] encapsulated within nano-hybrids made from self-assembling amphiphilic PAA-PS block co-polymers with silica shell cross-linkages. More recently, morphology-tailoring of a red AIEgen (aggregation-induced emission) bioprobe from microsized rods to nanospheres for tumor-targeted bioimaging was also developed by the same group [29]. All these advantages mentioned above, together with the potentially high fluorescent brightness [30], make the silica nanoparticles very desirable for bioimaging.

Here we report the synthesis and characterization of a biocompatible IR 780 loaded Pluronic-silica nanoparticles (IR780@NPs) as well its feasibility for *in vivo* imaging. The IR780@NPs were about 30 nm in size and displayed good monodispersity and stability. *In vitro* MTT assay on HEK293 and A431 cell lines demonstrated excellent biocompatibility of the IR780@NPs. In addition, fluorescent signal and retention time of IR780@NPs were much better than those of free dye during *in vivo* lymph node and tumor imaging. Combined with our novel synthesis pathway, IR780@NPs possess several remarkable features for *in vivo* bioimaging applications: (i) they can be readily prepared with varying concentrations of fluorescent dyes through our one-pot strategy; (ii) cross-linking can be realized, helping the nanoparticles maintain structural stability after dilution in blood; (iii) they have excellent water solubility, NIR fluorescence and photo- and chemical stability; (iv) they are

biocompatible and can be effectively internalized by cells; and (v) their size is ~30 nm, which is optimal for sentinel lymph node imaging and suitable for tumor imaging in deep tissues. Furthermore, the hydroxyl groups on the surface of IR780@NPs can be conjugated with biological molecules for active targeting. Therefore, these biocompatible NIR fluorescent Pluronic-silica nanoparticles are promising for *in vivo* bioimaging, therapy and intelligent drug delivery.

2. Materials and Methods

2.1. Materials

Pluronic F-127(PEO_{100}-PPO_{65}-PEO_{100}, average M_W ~12,600) was obtained from BASF Corp (Mount Olive, NJ). Tetraethyl ortosilicate (TEOS, 99.99%), diethoxydimethylsilane (DEDMS, 97%) and IR-780 iodide were purchased from Sigma-Aldrich Corp (St. Louis, MO). Hydrochloric acid (37%) and chloroform were purchased from Sigma Carlsbad, CA. Dulbecco's modified Eagle's medium (DMEM), streptomycin/penicillin, trypsin, fetal bovine serum (FBS) and all other cell culture supplements were purchased from Invitrogen (Carlsbad, CA). All reagents and solvents were used as received without further purification.

2.2. Preparation of IR780 loaded nanoparticles

In a typical preparation, 100 mg of Pluronic F127 and 0.5 mg of the IR780 iodide were carefully co-solubilized with 2 mL of dichloromethane in a 20 mL glass scintillation vial. The solvent was evaporated by means of a gentle nitrogen flow and subsequently placed under vacuum at room temperature. The solid residue was then solubilized under magnetic stirring with 1560 μL of 0.85 M HCl. The undissolved materials were discarded after centrifugation and the supernatant solution was transferred into a new 20 mL glass scintillation vial. TEOS (180 μL, 0.81 mmol) was then added to the resulting aqueous solution followed by DEDMS (15 μL, 0.09 mmol) after 120 min. The mixture was continuously stirred for 20 h at 25 °C before dialysis. The mixture was then placed in a dialysis bag (cutoff M_n: 3.5 kDa) and dialyzed against water for 48 h to remove free IR780 iodide. The water was replaced every 6 h, and finally, the mixture in the dialysis bag was freeze-dried to give a sponge-like powder.

To determine the loading efficiency of IR 780, lyophilized IR 780 nanoparticles were dissolved in dimethyl sulfoxide (DMSO) and measured by UV-NIR spectrometer (DU730, Beckman, USA) at 792 nm. All measurements were performed in triplicate. Dye loading efficiency (DLE) was calculated according to the following formula:

$$\mathrm{DLE\,(wt.\ \%)} = (\text{weight of loaded dye} / \text{weight of dye in feed}) \times 100\%$$

2.3. Characterization of IR780 loaded nanoparticles

Dynamic light scattering (DLS) measurements—The size and size distribution of IR780@NPs were determined using DLS at 25 °C on a Malvern ZS90 size analyzer at a 90° scattering angle. All samples were prepared in deionized water at a concentration of 0.5 mg mL^{-1}.

Transmission electron microscopy (TEM)—To further examine the morphology of the nanoparticles, a Philips F20 transmission electron microscopy (TEM) was used. The diluted NPs solution was dropped on a 400 mesh carbon coated copper grid and dried at room temperature. TEM imaging of the sample was performed at an acceleration voltage of 100 KV. To determine the nanoparticle size, over 100 particles were counted in multiple TEM images over different areas of the sample.

2.4. Optical property and stability of the IR780@NPs

The fluorescence spectra of IR 780 and the IR780@NPs were measured with a fluorescence spectrophotometer (DU730, Beckman, USA) at excitation wavelength of 780 nm, where both excitation and emission slits were set at 5 nm. To measure long-term fluorescent stability, aqueous solutions were prepared and placed in the dark at 25 °C. The fluorescence emission spectra were measured at predetermined intervals. The peak fluorescent intensity (at λ_{em} = 810 nm) of each sample was normalized by the corresponding fluorescence emission at time zero. The average normalized fluorescence intensity for each of the triplicate was plotted as a function of time.

2.5. Comparison of the fluorescence intensity of IR780@NPs and free dye

Florescence images were obtained by a Xenogen IVIS optical imaging device (PerkinElmer Inc.). For *in vitro* experiments, the IR780@NPs and free IR 780 were kept in the 1.5 mL eppendorf tubes. NIR fluorescence images of these samples were acquired using a 780 nm excitation light source and an 845 nm band-pass emission filter (with a 0.02 s exposure time).

To further confirm this fluorescence intensity in tissue, we carried out an intradermal injection experiment on a mouse model. Mice were injected with IR780@NPs (right back) and free dye (left back) formulations (50 μL, 5 μg/mL of dye eq.). Both sites were imaged by the Xenogen IVIS system. Mice were anesthetized with isoflurane and remained under anesthesia during the imaging procedure.

2.6. *In vitro* biocompatibility assay

The *in vitro* cytotoxicity of IR780@NPs was assessed with a methyl tetrazolium (MTT) viability assay against HEK 293 cells and A431 cells, following the established procedure [31]. The cells were seeded in 96-well plates at 10,000 cells per well. 100 μL of modified Eagle's medium (DMEM) containing 10% fetal bovine serum, supplemented with 100 U mL^{-1} penicillin and 100 U mL^{-1} streptomycin, was incubated at 37 °C in 5% CO_2 atmosphere for 24 h. NPs solution with different concentrations were added to each well, and the cells were subjected to MTT assay after being incubated for another 24 h or 48 h.

2.7. Intracellular uptake

The cellular uptake behaviours of IR 780 and IR780@NPs in A431 cells were determined by microscopy imaging with an NIR filter set (49030 ET, Chroma Technology Corp., excitation 775/50 nm, emission 845/55 nm). The cells were seeded in 6-well plates at ~2×10^5 cells per well in 2 mL complete DMEM media containing 10% fetal bovine serum, supplemented with 100 U mL^{-1} penicillin and 100 U mL^{-1} streptomycin, and incubated at

37 °C in 5% CO_2 atmosphere for 24 h. Then the cells were incubated for an additional 1 h with IR 780 and IR780@NPs at a final IR 780 concentration of 2.0 mg L^{-1} in complete DMEM, separately. Thereafter, the culture medium was removed and cells were washed with PBS three times. After that the cells were fixed with 4% paraformaldehyde for 30 min at room temperature, and the cell nuclei were stained with 4′, 6-diamidino-2-phenylindole (DAPI, blue). Fluorescence images of the cells were obtained with a Zeiss Axiovert 200 microscope.

2.8. *In vivo* lymph node imaging and tumor imaging

The female NCR nude mice, 7–9 weeks of age and with an average weight of about 25 g, were obtained from Taconic Farmer (One Hudson City Centre, Hudson). The animal experimental procedures in this study were approved by the Institutional Animal Care and Use Committee at the Johns Hopkins University.

Lymph node imaging *in vivo*—For *in vivo* lymph node imaging, the NCR nude mice were anesthetized with 250 μL of Ketamine/xylazine solution. Thereafter, 50 μL IR780@NPs and free dye (5 μg/mL, 250 ng IR-780 eq.) were administered intradermally into the forepaw pad for each mouse (n=3). 2 and 15 minutes after the injection, each mouse was imaged by the IVIS imaging system using a 780 nm excitation light source and an 845 nm band-pass emission filter (with a 0.02 s exposure time). All images were processed with the IVIS software.

Tumor imaging *in vivo*—Tumor-bearing mice were used for testing tumor imaging with the IR780@NPs *in vivo*. A human epidermoid carcinoma cancer xenograft tumor model was generated by subcutaneous injection of A431 cells (2×10^6) suspended in 100 μL PBS in the right flank of each mouse. About two weeks later, tumor nodules were visually observed on the mice. For each mouse, the initial tumor length (a, mm) and width (b, mm) were measured using a caliper and the tumor volume (V, mm^3) was calculated by the formula $V = ab^2/2$.

When the tumor volumes reached about ~200 mm^3, six tumor-bearing mice were randomly selected and divided into two groups, followed by tail vein injection with free dye (0.12 mg/kg) and IR780@NPs (0.12 mg/kg IR780 eq.). *In vivo* images were taken at indicated time points after injection using the *in vivo* IVIS imaging system. The nude mice were sacrificed at the 7th day after injection. The organs including lung, heart, liver, spleen, kidney and tumor were then collected immediately after euthanasia, followed by rinsing with physiological saline three times for *ex vivo* imaging. The results were analyzed by the IVIS software.

3. Results and Discussions

3.1. Synthesis and characterization of IR780@NPs

IR-780 iodide, a hydrophobic cation heptamethine dye with excellent optical and biocompatible properties, could be loaded into nanoparticles to increase its solubility in water. As shown in Scheme 1, the amphiphilic triblock copolymer Pluronic F127, composed

of poly(ethylene oxide) [PEO]-poly(propylene oxide) [PPO]-poly(ethylene oxide) [PEO], which can spontaneously self-assemble into micelles in an aqueous solution with a hydrophobic core and hydrophilic corona, was utilized as a template for creating spherical micelles. The micelles with encapsulated IR780 molecules were prepared from Pluronic F127 by the film rehydration method. After the sequential addition of the silane coupling agent TEOS and the cross-linking reagent DEDMS to the micellar solution, highly water-soluble IR 780 loaded nanoparticles (IR780@NPs) were obtained (Scheme 1). The dye loading efficiency for IR780 was calculated to be 74.9 % as measured by UV-NIR spectrometer. As can be seen in Figure 1A, the IR780@NPs showed discrete and uniform spherical structures with a diameter of ~25 nm. The average hydrodynamic diameter of the as-synthesized silica NPs was approximately 30 nm with a PDI of 0.118 as measured by DLS (Figure 1B), which correlates well with the result from TEM imaging. In addition, all particles were well dispersed with almost no aggregation, signifying that there were no inter-particle interactions caused by the cross-linking reaction within the micelles. Moreover, the obtained nanoparticle size would be an extra benefit for deep penetration into tumor tissue [32]. Compared to the previously reported techniques for preparing dye loaded silica nanoparticles, this one-pot synthesis strategy has distinct advantages such as low cost, simple and controllable preparation process and adjustable dye loading amount. Moreover, this nanoparticle fabrication platform can also be easily adapted for drug delivery systems by replacing the dyes with anti-cancer drugs.

3.2. Optical properties and stability of the IR780@NPs

In order to verify the successful encapsulation of the IR780 molecules into the nanoparticles without denaturation, the optical properties of IR780@NPs including absorption and emission were investigated. As shown in Figure 2, the wavelength of the maximum absorption from IR780@NPs was red-shifted by approximately 20 nm compared to free dye (Figure 2A). The emission spectra of IR780@NPs exhibited a similar red-shift by approximately 15 nm to 815 nm (Figure 2B). This distinct red-shift clearly demonstrated that IR780 was successfully encapsulated into the silica nanoparticles, rather than physically adsorbed onto the surface of the shell. In addition, the fluorescence intensity of the IR780@NPs solution remained the same for up to a month (Figure 2C), while the fluorescence intensity of free dye solution rapidly declined to only 35% of its initial intensity after one week, and 6% after one month. Over the course of one month, it was also noted that there was no precipitation and that the size of the IR780@NPs remained constant at 30 nm (Figure 2D), thus indicating that there was no aggregation in the aqueous solution. These results support our assertion that IR780@NPs are more optically and chemically stable than free IR780 dye, making them promising for *in vivo* bioimaging.

3.3. Biocompatibility of nanoparticles

Since cytotoxicity is a serious concern for *in vivo* bioimaging, cellular biocompatibility experiments were carried out using MTT assay with A431 (human epidermoid carcinoma cells) and HEK 293 (normal human embryo kidney cells) as test cell lines. Both cells were incubated with blank silica nanoparticles and IR780@NPs at gradient concentrations from 0.0325 to 1.0 mg mL^{-1} for 24 h and 48 h. As shown in Figure 3, the cell viability after 24 h and 48 h of incubation were all above 90% even at the highest concentration of 1.0 mg

mL^{-1}, indicating low toxicity and good biocompatibility of the silica nanoparticles to normal and tumour cells.

3.4. Intracellular uptake of IR780@NPs

To evaluate the potential of IR780@NPs for intracellular imaging, internalization of IR780@NPs by A431 cells was observed using fluorescence microscopy. As shown in Figure 4, red fluorescence appeared in all cells after incubation with IR780@NPs for 1 h, indicating that the nanoparticles were successfully internalized by cancer cells. This suggests that the nanoparticles can be an efficient nanocarrier to deliver dyes/drugs into cancer cells. Notably, the intracellular IR780 fluorescence intensity from IR780@NPs was much stronger than that of free IR780 at the same incubation time, suggesting that IR780@NPs can be employed as a high quality NIR fluorescent contrast agent for cellular imaging.

3.5. Comparison of fluorescence intensity of IR780@NPs and free IR780 dye

It is well known that a high fluorescent signal will improve the signal-to-noise ratio for *in vivo* imaging. By characterizing the photo-physical behaviour of IR780@NPs, we have demonstrated that the silane coupling agent played a critical role in achieving the stable fluorescence property of the nanoparticles. It would be critical to compare the fluorescence brightness of these particles with free dye. Figures 5A and 5B show the quantitative and qualitative fluorescence intensity of IR780@NPs and free dye at different concentrations, respectively. The fluorescence signals of IR780@NPs were much higher than that of free dye at the same concentration. The brightness enhancement may be attributed to the protection of the fluorophores from the solvent upon addition of the silica shell [24]. To further confirm our observations, *in vivo* fluorescence imaging experiments on a mouse model were performed with subcutaneous injection of IR780@NPs and free IR780 dye solutions. As shown in Figures 5C and 5D, the fluorescence intensity of IR780@NPs was obviously higher than the free dye alone (by about 5–6 fold), suggesting that the bright IR780@NPs could also offer a much better fluorescence penetration depth for deep tissue imaging.

3.6. Sentinel lymph node imaging

Sentinel lymph node (SLN) mapping has been widely used in clinic to predict the metastatic spread of a primary tumor to regional lymph nodes [9]. IR-780 iodide, which has a higher fluorescence emission and many unique optical advantages over Indocyanine green (ICG), has been already applied for sentinel lymph nodes (SLNs) mapping in animal models [7]. IR780@NPs, with a hydrodynamic diameter of about 30 nm (an optimal size for lymph node uptake [9]) and excellent fluorescence brightness, can be particularly suited for SLN mapping. For this purpose, an *in vivo* SLN imaging experiment was performed on a mouse model. IR780@NPs and free dye solutions were injected into the left forepaw of separate mice and the fluorescence images were taken using the IVIS system after the intradermal injection. As we can see from Figures 6A and 6B (and the insets), fluorescence was observed around the sentinel lymph node of the mouse injected with IR780@NPs at about 2 min. Though the fluorescence intensity diminished, it was still visible even 15 min post injection. In comparison, under the same experimental conditions, the fluorescence signal of

the SLN of the mouse injected with free IR780 after 15 min was nearly undetectable (see Figures 6C and 6D and the insets). It was also noted in Figure 6 that the fluorescence signal at the injection site on the left forepaw was much stronger with the IR780@NPs than with free dye at the same time point (2 min and 15 min post injection, respectively). It can be inferred that the relatively weak fluorescence of IR780 (Figures 6C and 6D) in SLN is due to its small size; the free dye can easily diffuse from the SLN into other lymph nodes [9], while the IR780@NPs were much larger and harder to migrate from SLN to other lymph nodes, resulting in stronger fluorescence signals and longer retention times for IR780@NPs in the SLN. This result indicates that IR780@NPs could be a promising contrast agent for *in vivo* SLN mapping.

3.7. Tumor imaging *in vivo*

To further explore other possible biomedical applications, we investigated the nanoparticles for tumor imaging on a xenografted mouse cancer model. A431 cells were subcutaneously implanted on the right flank of female NCR nude mice. When the tumors reached ~200 mm^3, the mice were given a single intravenous injection of either an IR780@NPs solution or a free IR780 dye solution (n = 3 per group), whereas the free dye served as a control. Since most solid tumors exhibit hypervascularity, leaky vascular architecture and the absence of effective lymphatic drainage, macromolecules and nanometer-sized particles can accumulate preferentially at tumour sites through a passive targeting effect, known as Enhanced Permeability and Retention effect (EPR effect)[33, 34]. To verify whether IR780@NPs can preferentially accumulate in tumors *in vivo*, the tumor-bearing mice were imaged by the IVIS system at specified time intervals from 2 to 144 h post-injection. Mice before injection were also imaged as calibration. As we can see from Figure 7A, the signal intensity after the IR780@NPs injection reached the maximum at ~48 h, while signal from the free IR780 dye injection reached its maximum at ~12 h. Tumor-bearing mice injected with free dye showed almost no detectable signal after 144 h; however, the signal from the mice injected with IR780@NPs was still visible. It is also clear that the tumor florescence signal of IR780@NPs was much higher than that of the free dye during the whole imaging period, which was probably attributed to the combination of EPR effect and enhanced brightness of the IR780@NPs (as shown in Figure 5A). In order to quantify the time-dependent distribution, the average signal over the tumor area was plotted against time in Figure 7B. It can be seen that the maximum accumulation of IR780@NPs and IR780 was achieved at 36 and 12 h post injection, respectively, indicating that IR780@NPs has a much longer blood circulation time.

The mice were sacrificed after imaging at 144 h post injection. Different organs were excised and then imaged with the IVIS system. Figure 8A shows the fluorescence images of all excised organs and the tumor on the same intensity scale, with red representing the lowest intensity and yellow representing the highest. The fluorescence intensity of IR780@NPs in the tumor is clearly higher than that of free dye. The intensity distribution in each organ was also quantitatively illustrated in Figure 8B. As we can see, the fluorescence intensity from the tumor injected with IR780@NPs after 144 h is almost 6 times as high as the one injected with free IR780 dye, which is consistent with the results shown in Figure 7B.

IR780@NPs shown here have a strong signal and high contrast between the tumor and surrounding tissues during this long-term NIR imaging experiment. As we expected, the free dye had rapid clearance and its signal was relatively weak. The data provides strong evidence that IR780@NPs are sufficient for long term *in vivo* tumor imaging.

4. Conclusion

We successfully designed and synthesized silica-Pluronic hybrid nanoparticles. IR780 as a model dye was loaded into the nanoparticles by a facile one-pot strategy. The structures of the obtained IR780-loaded nanoparticles (IR780@NPs) were carefully investigated. The nanoparticles were monodisperse with a spherical shape and a diameter of about 30 nm. Experimental results showed that IR780@NPs are stable over a long period of time without aggregation (at least one month) and that IR780@NPs dramatically improve the photo-stability of IR780. Moreover, the IR780@NPs showed a higher brightness compared to free dye. Notably, *in vitro* MTT assay demonstrated excellent biocompatibility of the nanoparticles both before and after loading with IR780 dye molecules. Most importantly, the IR780@NPs exhibited excellent characteristics for imaging with a long circulation time and high retention in tumor and SLNs. Overall, our results suggest that the IR780@NPs might represent a promising class of fluoroprobes as a contrast agent for *in vivo* imaging, and potentially for therapy and drug delivery.

Acknowledgments

This work was supported in part by the National Institutes of Health (NIH) under grants R01 CA120480, R01 CA153023, and U54CA151838, and the National Science Foundation (NSF) under grant CBET-1430040.

References

1. Ntziachristos V. Nat Methods. 2010; 7:603–614. [PubMed: 20676081]
2. Jones SA, Shim SH, He J, Zhuang XW. Nat Methods. 2011; 8:499–U496. [PubMed: 21552254]
3. Licha K, Olbrich C. Adv Drug Deliver Rev. 2005; 57:1087–1108.
4. Janib SM, Moses AS, MacKay JA. Adv Drug Deliver Rev. 2010; 62:1052–1063.
5. Jiang S, Gnanasammandhan MK, Zhang Y. J R Soc Interface. 2010; 7:3–18. [PubMed: 19759055]
6. Keereweer S, Van Driel PBAA, Snoeks TJA, Kerrebijn JDF, de Jong RJB, Vahrmeijer AL, Sterenborg HJCM, Lowik CWGM. Clin Cancer Res. 2013; 19:3745–3754. [PubMed: 23674494]
7. Zhang C, Wang SJ, Xiao J, Tan X, Zhu Y, Su YP, Cheng TM, Shi CM. Biomaterials. 2010; 31:1911–1917. [PubMed: 19963270]
8. Unno N, Nishiyama M, Suzuki M, Yamamoto N, Inuzuka K, Sagara D, Tanaka H, Konno H. Eur J Vasc Endovasc. 2008; 36:230–236.
9. Noh YW, Kong SH, Choi DY, Park HS, Yang HK, Lee HJ, Kim HC, Kang KW, Sung MH, Lim YT. ACS Nano. 2012; 6:7820–7831. [PubMed: 22862428]
10. Na JH, Koo H, Lee S, Min KH, Park K, Yoo H, Lee SH, Park JH, Kwon IC, Jeong SY, Kim K. Biomaterials. 2011; 32:5252–5261. [PubMed: 21513975]
11. Ferber S, Baabur-Cohen H, Blau R, Epshtein Y, Kisin-Finfer E, Redy O, Shabat D, Satchi-Fainaro R. Cancer Lett. 2014; 352:81–89. [PubMed: 24614283]
12. Frangioni JV. Curr Opin Chem Biol. 2003; 7:626–634. [PubMed: 14580568]
13. Hilderbrand SA, Weissleder R. Curr Opin Chem Biol. 2010; 14:71–79. [PubMed: 19879798]
14. Zheng XH, Zhou FF, Wu BY, Chen WR, Xing D. Mol Pharmaceut. 2012; 9:514–522.
15. Qi LF, Gao XH. Expert Opin Drug Del. 2008; 5:263–267.

16. Ghoroghchian PP, Frail PR, Susumu K, Blessington D, Brannan AK, Bates FS, Chance B, Hammer DA, Therien MJ. P Natl Acad Sci USA. 2005; 102:2922–2927.
17. Rodriguez VB, Henry SM, Hoffman AS, Stayton PS, Li XD, Pun SH. J Biomed Opt. 2008; 13:014025. [PubMed: 18315383]
18. Chen YP, Li XD. Biomacromolecules. 2011; 12:4367–4372. [PubMed: 22040128]
19. Torchilin V. Adv Drug Deliver Rev. 2011; 63:131–135.
20. Hardman R. Environ Health Persp. 2006; 114:165–172.
21. Park K, Lee S, Kang E, Kim K, Choi K, Kwon IC. Adv Funct Mater. 2009; 19:1553–1566.
22. Yu J, Yaseen MA, Anvari B, Wong MS. Chem Mater. 2007; 19:1277–1284.
23. Lee CH, Cheng SH, Wang YJ, Chen YC, Chen NT, Souris J, Chen CT, Mou CY, Yang CS, Lo LW. Adv Funct Mater. 2009; 19:215–222.
24. Huo QS, Liu J, Wang LQ, Jiang YB, Lambert TN, Fang E. J Am Chem Soc. 2006; 128:6447–6453. [PubMed: 16683810]
25. Yuan JJ, Mykhaylyk OO, Ryan AJ, Armes SP. J Am Chem Soc. 2007; 129:1717–1723. [PubMed: 17249673]
26. Wu XM, Chang S, Sun XR, Guo ZQ, Li YS, Tang JB, Shen YQ, Shi JL, Tian H, Zhu WH. Chem Sci. 2013; 4:1221–1228.
27. Chang S, Wu XM, Li YS, Niu DC, Ma Z, Zhao WR, Gu JL, Dong WJ, Ding F, Zhu WH, Shi JL. Adv Healthc Mater. 2012; 1:475–479. [PubMed: 23184780]
28. Chang S, Wu XM, Li YS, Niu DC, Gao YP, Ma Z, Gu JL, Zhao WR, Zhu WH, Tian H, Shi JL. Biomaterials. 2013; 34:10182–10190. [PubMed: 24095249]
29. Li YS, Shao AD, Wang Y, Mei J, Niu DC, Gu JL, Shi P, Zhu WH, Tian H, Shi JL. Adv Mater. 2016; 28:3187–3193. [PubMed: 26917199]
30. Sokolov I, Naik S. Small. 2008; 4:934–939. [PubMed: 18581411]
31. Yan LS, Yang LX, He HY, Hu XL, Xie ZG, Huang YB, Jing XB. Polym Chem-Uk. 2012; 3:1300–1307.
32. Cabral H, Matsumoto Y, Mizuno K, Chen Q, Murakami M, Kimura M, Terada Y, Kano MR, Miyazono K, Uesaka M, Nishiyama N, Kataoka K. Nat Nanotechnol. 2011; 6:815–823. [PubMed: 22020122]
33. Matsumura Y, Maeda H. Cancer Res. 1986; 46:6387–6392. [PubMed: 2946403]
34. Maeda H, Wu J, Sawa T, Matsumura Y, Hori K. J Control Release. 2000; 65:271–284. [PubMed: 10699287]

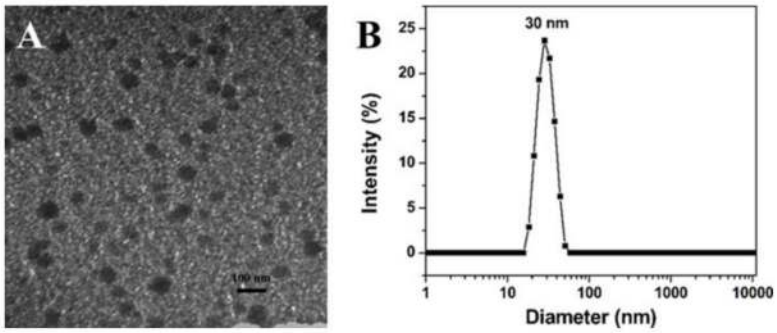

Figure 1.

Characterization of IR780@NPs. (A) TEM image of IR780@NPs. (B) Size and size distribution of IR780@NPs by dynamic light scattering (DLS).

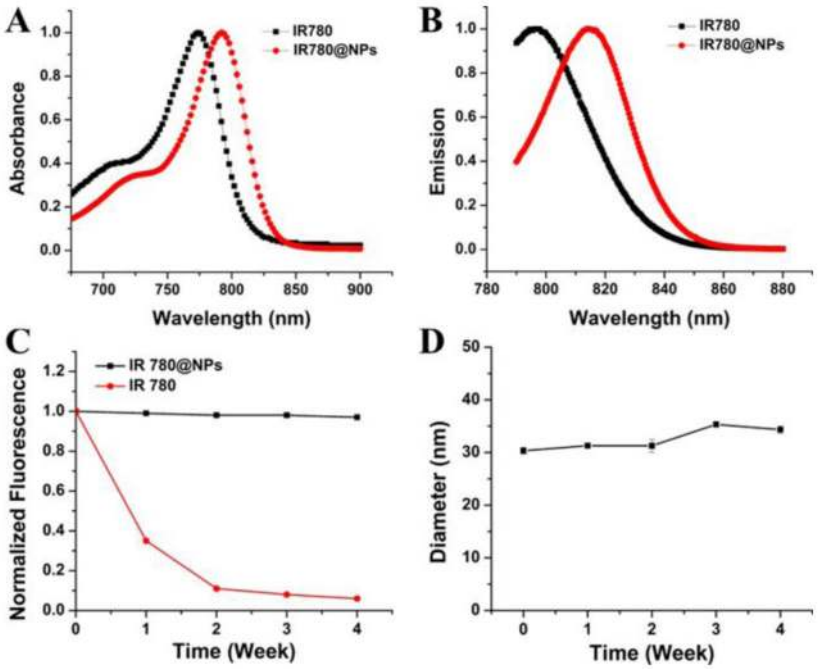

Figure 2.

(A) Normalized absorption spectra and (B) emission spectra of IR780@NPs and free IR780. (C) Fluorescence stability of IR780@NPs and free IR780 solutions. (D) Size stability of IR780@NPs in aqueous solution.

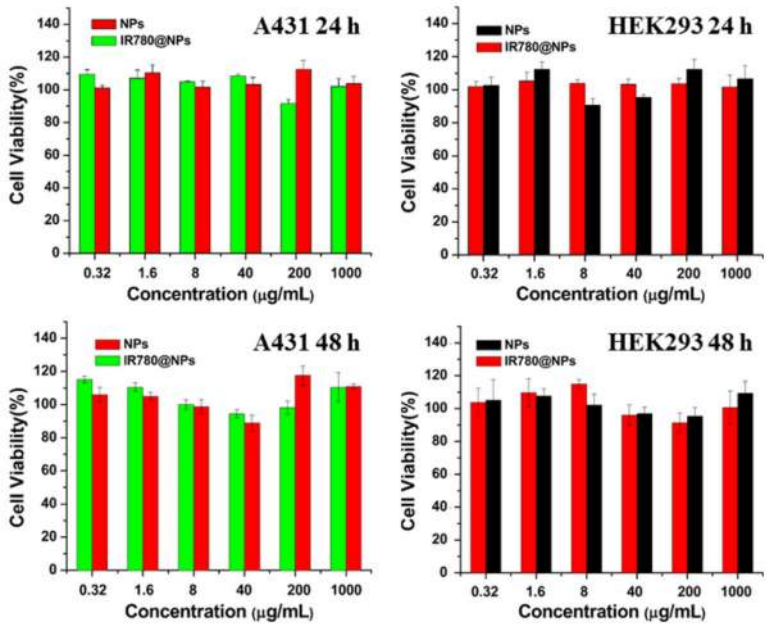

Figure 3.

Cell viability on A431 and HEK293 cell lines after 24 h or 48 h incubation with blank silica nanoparticles and IR780@NPs.

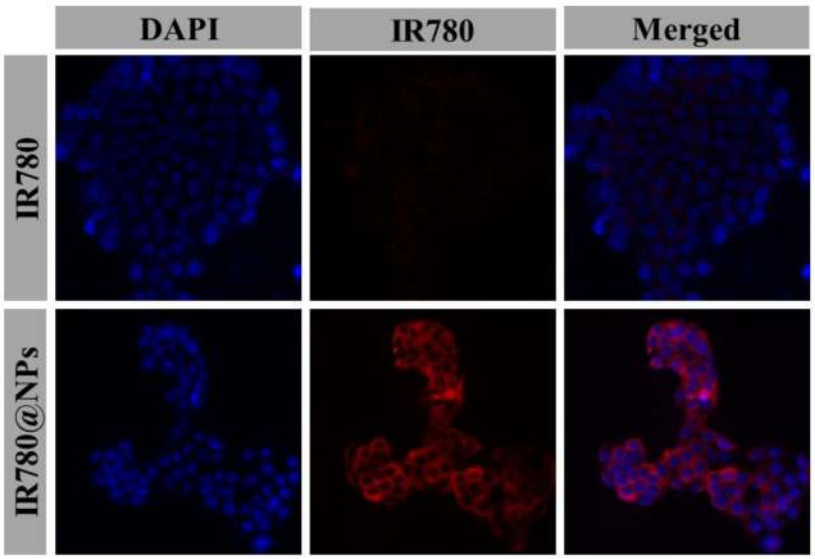

Figure 4.

Fluorescence microscopy images of A431 cells incubated with free IR780 dye and IR780@NPs for 1 h. Cell nuclei were stained by DAPI (blue) and NIR fluorescence of IR780 was marked in red.

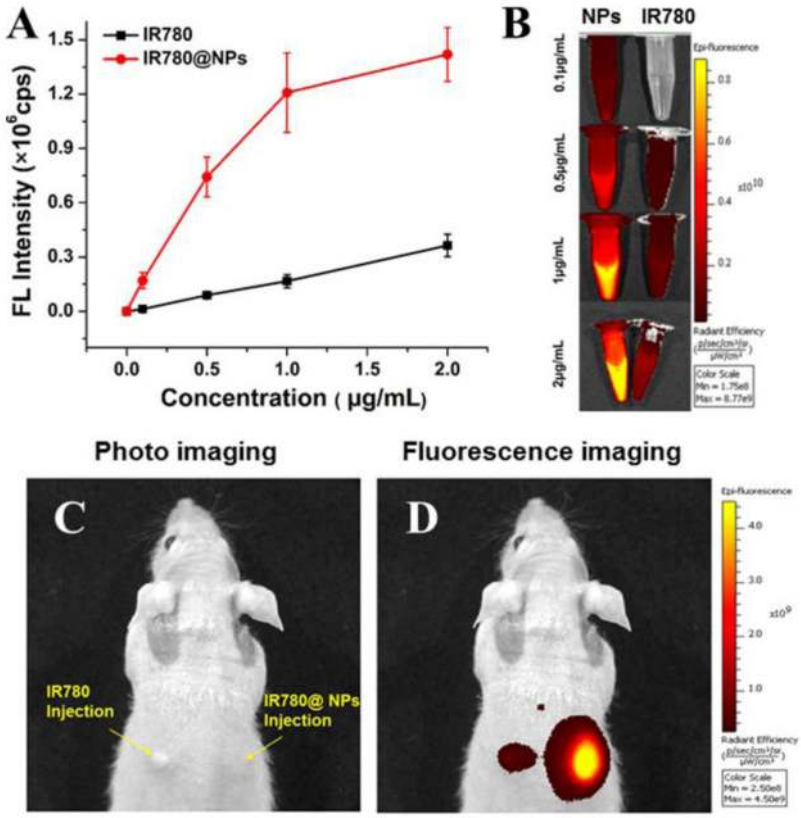

Figure 5.

Comparison of fluorescence intensity between IR780@NPs and free IR780 dye. (A) Plots of fluorescence intensity versus concentration. (B) Fluorescence image of IR780@NPs and free dye at different concentrations. (C) Photo of a mouse after subcutaneous injection of IR780@NPs and free IR780 dye solutions. (D) Fluorescence image of the mouse after subcutaneous injection by IVIS post subcutaneous injection.

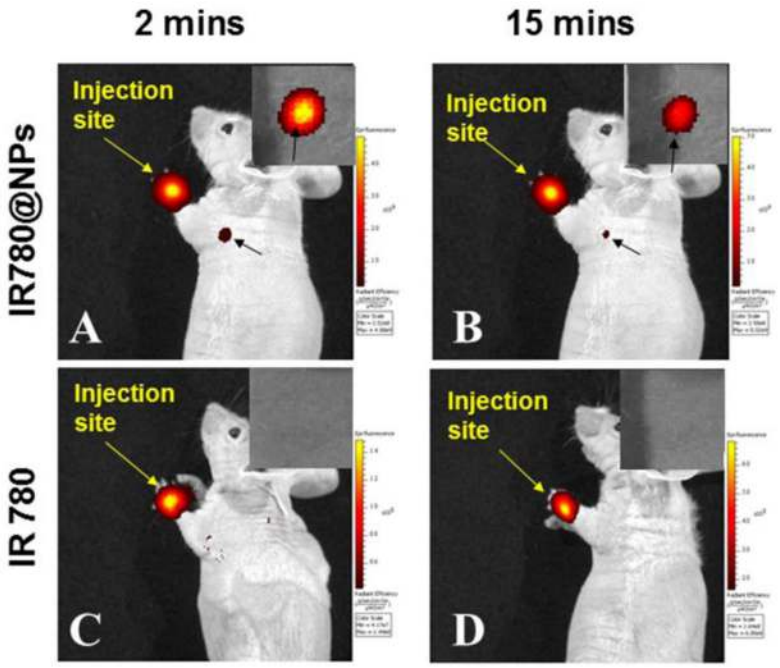

Figure 6.
Sentinel lymph node fluorescence imaging after intradermal injection of IR780@NPs and free dye IR780.

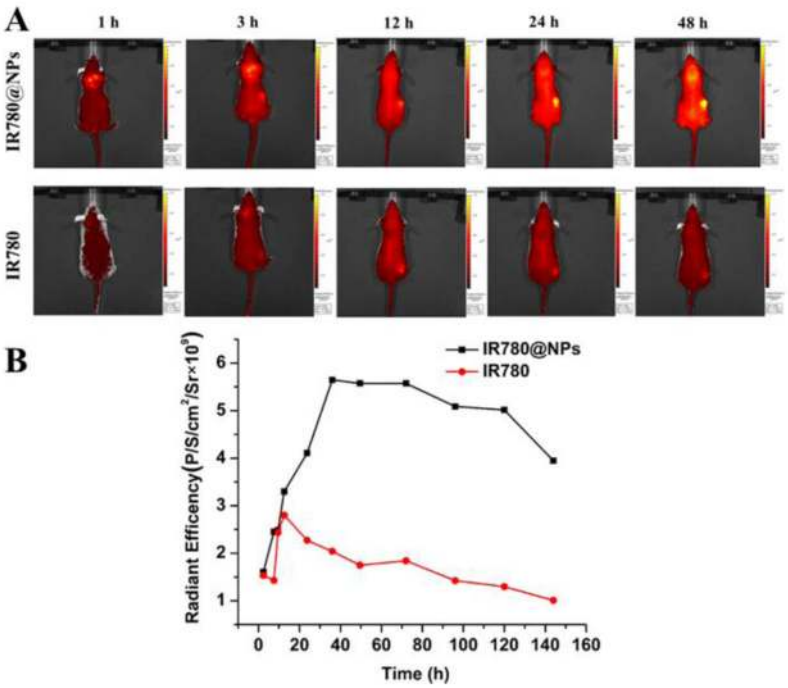

Figure 7.

In vivo fluorescence imaging of tumour-bearing (A431) nude mice after tail-vein injection of IR780@NPs and free dye IR 780 solutions. (A) *In vivo* images taken at different time points. (B) Average NIR signals collected from the tumour site as a function of time.

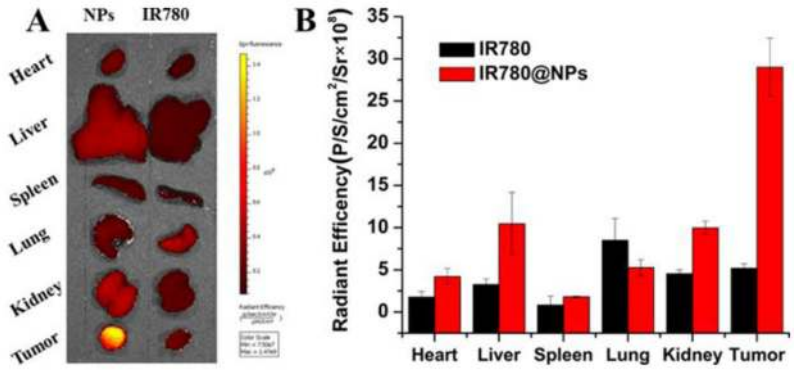

Figure 8.

(A) Fluorescence images of various organs of nude mice 144 h after tail-vein injection of IR 780 and IR780@NPs at an equivalent dose of IR780 (0.12 mg kg^{-1} bodyweight). (B) Quantitative average signals from different organs and the tumour.

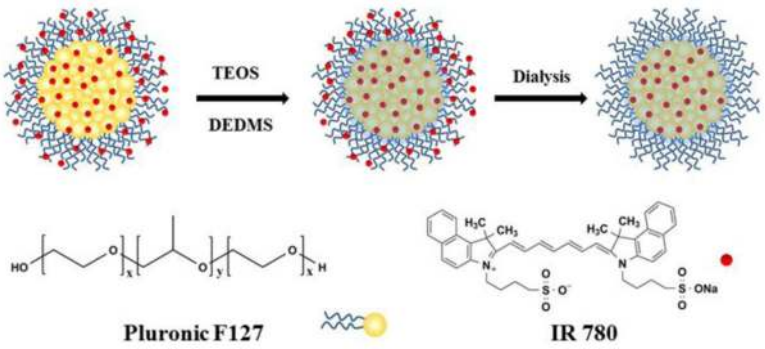

Scheme 1.

The schematic illustration of preparation of the NIR fluorescent silica-Pluronic F127 core-shell nanoparticles (IR780@NPs).